Vol 18 No 7, July 2009
1674-1056/2009/18(07)/2749-08

Chinese Physics B

© 2009 Chin. Phys. Soc.
and IOP Publishing Ltd

Small-signal analysis of a rectangular helix structure traveling-wave-tube*

Fu Cheng-Fang(付成芳)†, Wei Yan-Yu(魏彦玉)‡, Duan Zhao-Yun(段兆云),
Wang Wen-Xiang(王文祥), and Gong Yu-Bin(宫玉彬)§

National Key Laboratory of High Power Vacuum Electronics, University of Electronic Science and Technology of China, Chengdu 610054, *China*

(Received 18 October 2008; revised manuscript received 10 November 2008)

This paper investigates the properties of traveling wave-beam interaction in a rectangular helix traveling-wave-tube (TWT) for a solid sheet electron beam. The 'hot' dispersion equation is obtained by means of the self-consistent field theory. The small signal analysis, which includes the effects of the beam parameters and slow-wave structure (SWS) parameters, is carried out by theoretical computation. The numerical results show that the bandwidth and the small-signal gain of the rectangular helix TWT increase as the beam current increases; and the beam voltage not obviously influences the small signal gain. Among different rectangular helix structures, the small-signal gain increases as the width of the rectangular helix SWS increases, however, the bandwidth decreases whether structure parameters a and L or ψ and L are fixed or not. In addition, a comparison of the small-signal gain of this structure with a conventional round helix is made. The presented analysis will be useful for the design of the TWT with a rectangular helix circuit.

Keywords: rectangular helix, small-signal gain, slow-wave structure, compact TWT
PACC: 4110, 4170, 7870G

1. Introduction

With the requirement of a large number of compact traveling-wave-tubes (TWTs) in millimeter wave radar, communications and electronic-warfare, a fabrication technique named micro-electro-mechanical systems (MEMS) has widely attracted scholars' interest due to some of its peculiarities: increased reliability, improved repeatability, small tolerances, batch yields and reduced cost, which make it worth consideration as an alternative TWT interaction design based on this fabrication technique.[1,2] For exciting microwave or millimeter wave energy in a wide frequency range, the slow-wave structure (SWS), a key component of the electron beam–wave interaction of a TWT, is required to possess weak dispersion and good thermal stability. For the conventional round helix SWS, its modifications and the coupled cavity SWS have met serious difficulties in satisfying these requirements simultaneously at the millimeter wave band. Thus, the investigation of novel compact slow-wave interaction structures based upon MEMS is more important.

A related helix structure in planar geometry was therefore considered in Refs.[2]–[7]. This structure, called the 'planar helix', consists of a pair of parallel infinitely unidirectionally conducting (UC) screens conducting in different directions and separated by some distance.[2−7] The unified dispersion equation and interaction impedance for different possibilities of fabricating the planar helix on dielectric substrates are obtained in Ref.[6]. Also a planar helix TWT based on this structure is proposed and the model solution is obtained in Ref.[7]. However, the structure studied in Refs.[2]–[7] is an ideal model which is taken to be infinitely wide in one direction, therefore, the influence of the width of the planar helix is ignored—a mathematical idealization which can be simply modeled. In our previous work we provide such a theory with a rigorous approach on the slow-wave characteristics for a general rectangular helix SWS in free space[8] and printed on dielectric substrates using the field-matching method.[9] The results reveal that the phase velocity decreases and interaction impedance increases at higher frequencies by flattening (increasing the aspect ratio of) the rectangular helix structure. And the rectangular helix SWS can achieve higher coupling

*Project supported in part by the National Natural Science Foundation of China (Grant No 60532010) and the Talent Fund of Chinese Education Administration.
†E-mail: fchf2006@uestc.edu.cn
‡E-mail: yywei@uestc.edu.cn
§E-mail: ybgong@uestc.edu.cn

impedance than the equivalent circular helix at comparable phase velocities. But to our knowledge, there is no work on the beam-wave interaction in the rectangular helix TWT. The purpose of this paper is to investigate the properties of traveling wave-beam interaction in a rectangular helix TWT for a solid sheet electron beam.

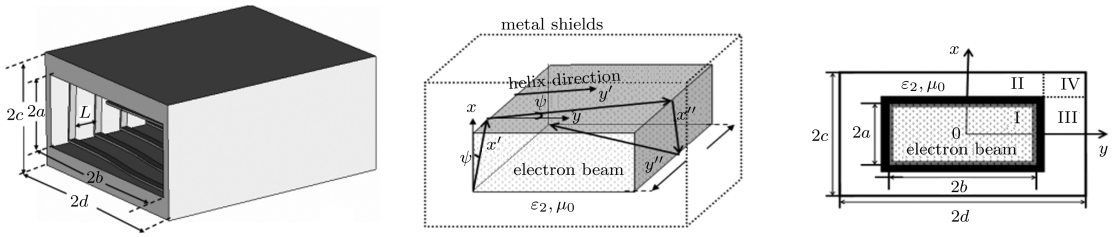
In this paper, we present a linear analysis of the beam-wave interaction for the rectangular helix SWS loading with a linear sheet electron beam. The 'hot' dispersion equation is derived by applying the self-consistent field theory and the electromagnetic integral equations at the SWS's boundaries.[10−12] Then the influence of the beam parameters and structure parameters on the small-signal gain are investigated and discussed based upon the numerical calculation. At the same time the comparison of small signal gain of this structure with a conventional round helix is made.

This paper is organized as follows. In Section 2, by means of the self-consistent field theory, the field distributions of each region in the structure are derived; then, by utilizing boundary conditions at the edges of the structure and the beam, the 'hot' dispersion equation of this structure is obtained. In Section 3, the influences of the beam parameters and the structure parameters on the small-signal gain are investigated numerically. At the same time the small-signal gain per period of the rectangular helix TWT are compared with a conventional round helix TWT. Finally, a brief discussion is given in Section 4.

2. The 'hot' dispersion equation of beam-wave interaction

2.1. Configuration

The configuration of the rectangular helix considered here is shown in Fig.1, and can be described in terms of a rectangular coordinate system (x, y, z), where $2a$ and $2b$ are the height and width of the rectangular SWS cross section, respectively, $2c$ and $2d$ are the height and width, of the rectangular shield screen respectively, L is the pitch, and ψ is the pitch angle. Just as Refs.[12] and [13] in 'sheath helix' approximation, the four side surfaces are represented as UC screens, which are separated by a distance $2a$ in the x-direction and $2b$ in the y-direction (Fig.1(b)).



(a) (b)

Fig.1. (a) A schematic view of a rectangular helix TWT. (b) The rectangular helix TWT analytic model.

For the convenience of analysis, a sheet electron beam with a rectangular cross section of height $2a$ and width $2b$ is located inside the rectangular helix SWS. The sheet electron beam employed here is assumed to be guided by an infinite magnetic field B_0 in the z-direction, thus, it propagates uniformly along the z-axis of the system with a velocity v_e. The beam current density is constant over the cross section and has only a z-component. In practice, this assumption is very nearly realized by means of the focusing action of a strong DC magnetic field applied in the z-direction.

Considering the symmetry of the rectangular helix together with Maxwell's equations, one finds that the solution of this problem must be either even or odd if x and y are taken in conjunction. Thus the structure admits two independent solutions: transverse-symmetric (even) modes and transverse- antisymmetric (odd) modes.[3] In the former type, the transverse field components are symmetrical with respect to x and y, while the longitudinal field components E_z and H_z are anti-symmetrical. Similarly, in the latter type of modes, the opposite is true. Finally, due

to the conducting boundary conditions of the rectangular helix being at finite angles from the transverse x–y plane, all the solutions in the helix with a rectangular cross section are hybrid modes (both TE and TM modes are required). The symmetry also ensures that only a quarter of the structure needs be considered for analysis. The quarter structure is divided into four regions for analysis: region I ($0 < x < a$ and $0 < y < b$); region II ($a < x < c$ and $0 < y < b$); region III ($0 < x < a$ and $b < y < d$) and region IV ($a < x < c$ and $b < y < d$). For simplification reasons in the following analysis, the weak fields in region IV are neglected. By solving the linear motion and continuity equations for the electron beam and the Maxwell equation for the perturbed field E and H in the linearized framework in a rectangular coordinate system, the field expressions in different regions can be obtained; then, the field expressions are substituted into the matching equations to get the 'hot' dispersion equation.

2.2. The field distributions

In region I, the electron beam region is regarded as a sheet of travelling plasma. Because of the influence of the electron beam, the wave number γ_{e} in the transverse direction of region I can be expressed as

$$\gamma_{\mathrm{e}}^2 = p_u^2 + p_v^2 = \varepsilon_{\mathrm{e}}(\beta^2 - k_0^2). \tag{1}$$

Here, β is the phase constant, while p_u and p_v are the propagation coefficients in the x-direction and y-direction, $k_0^2 = \omega^2\varepsilon_0\mu_0$ is the wave number in free space, ω is the angular frequency. The $\varepsilon_{\mathrm{e}} = 1 - \omega_{\mathrm{p}}^2/(\omega - \beta v_{\mathrm{e}})^2$ is the relative dielectric constant, where, $\omega_{\mathrm{p}} = \sqrt{(\rho_0 e/\varepsilon_0 m_{\mathrm{e}})}$ is the plasma frequency, $\rho_0 = J/v_{\mathrm{e}}$ is the density of electric charge, $v_{\mathrm{e}} = \sqrt{(2eV_0/m_{\mathrm{e}})}$ is the speed of electron, J is the current density, e is the electron charge, ε_0 is the vacuum permittivity, m_{e} is the static electron mass, I_0 and V_0 indicate the electron beam current and acceleration voltage, respectively. In regions II and III $\gamma_2^2 = u_i^2 + v_i^2 = \beta^2 - k_2^2, (i = 2, 3)$, $k_2^2 = \omega^2\varepsilon_{\mathrm{r}2}\varepsilon_0\mu_{\mathrm{r}}\mu_0$, where, u_i and v_i are the propagation coefficients in the x-direction and y-direction in regions II and III respectively.

The field expressions in each region can be obtained by solving the equations of motion, continuity of the electron beam, and Maxwell's equations in a rectangular coordinate system. The transverse field components can then be expressed in terms of the longitudinal components of the fields. Omitting $\mathrm{e}^{(\mathrm{j}\omega t - \mathrm{j}\beta z)}$, we can write all the field expressions as follows:

1) In region I ($0 < x < a$ and $0 < y < b$):

$$\begin{aligned}
E_{1z} &= A\cosh(p_u x)\cosh(p_v y),\\
H_{1z} &= B\cosh(p_u x)\cosh(p_v y),\\
E_{1x} &= \frac{\mathrm{j}\beta}{\gamma_{\mathrm{e}}^2}Ap_u\sinh(p_u x)\cosh(p_v y) + \frac{\mathrm{j}\omega\mu_0}{\gamma_{\mathrm{e}}^2}Bp_v\cosh(p_u x)\sinh(p_v y),\\
E_{1y} &= \frac{\mathrm{j}\beta}{\gamma_{\mathrm{e}}^2}Ap_v\cosh(p_u x)\sinh(p_v y) - \frac{\mathrm{j}\omega\mu_0}{\gamma_{\mathrm{e}}^2}Bp_u\sinh(p_u x)\cosh(p_v y),\\
H_{1x} &= -\frac{\mathrm{j}\omega\varepsilon_0}{\gamma_{\mathrm{e}}^2}Ap_v\cosh(p_u x)\sinh(p_v y) + \frac{\mathrm{j}\beta}{\gamma_{\mathrm{e}}^2}Bp_u\sinh(p_u x)\cosh(p_v y),\\
H_{1y} &= \frac{\mathrm{j}\omega\varepsilon_0}{\gamma_{\mathrm{e}}^2}Ap_u\sinh(p_u x)\cosh(p_v y) + \frac{\mathrm{j}\beta}{\gamma_{\mathrm{e}}^2}Bp_v\cosh(p_u x)\sinh(p_v y).
\end{aligned} \tag{2}$$

2) In region II ($a < x < c$ and $0 < y < b$):

$$\begin{aligned}
E_{2z} &= C\sinh(u_2(c - x))\cosh(v_2 y),\\
H_{2z} &= D\cosh(u_2(c - x))\cosh(v_2 y),
\end{aligned}$$

$$E_{2x} = -\frac{\mathrm{j}\beta}{\gamma_2^2} Cu_2 \cosh(u_2(c-x)) \cosh(v_2 y) + \frac{\mathrm{j}\omega\mu_0}{\gamma_2^2} Dv_2 \cosh(u_2(c-x)) \sinh(v_2 y),$$

$$E_{2y} = \frac{\mathrm{j}\beta}{\gamma^2} Cv_2 \sinh(u_2(c-x)) \sinh(v_2 y) + \frac{\mathrm{j}\omega\mu_0}{\gamma_2^2} Du_2 \sinh(u_2(c-x)) \cosh(v_2 y),$$

$$H_{2x} = -\frac{\mathrm{j}\omega\varepsilon_2}{\gamma_2^2} Cv_2 \sinh(u_2(c-x)) \sinh(v_2 y) - \frac{\mathrm{j}\beta}{\gamma_2^2} Du_2 \sinh(u_2(c-x)) \cosh(v_2 y),$$

$$H_{2y} = -\frac{\mathrm{j}\omega\varepsilon_2}{\gamma_2^2} Cu_2 \cosh(u_2(c-x)) \cosh(v_2 y) + \frac{\mathrm{j}\beta}{\gamma_2^2} Dv_2 \cosh(u_2(c-x)) \sinh(v_2 y). \tag{3}$$

3) In region III ($0 < x < a$ and $b < y < d$):

$$E_{3z} = E \cosh(u_3 x) \sinh(v_3(d-y)),$$

$$H_{3z} = F \cosh(u_3 x) \cosh(v_3(d-y)),$$

$$E_{3x} = \frac{\mathrm{j}\beta}{\gamma_2^2} Eu_3 \sinh(u_3 x) \sinh(v_3(d-y)) - \frac{\mathrm{j}\omega\mu_0}{\gamma_2^2} Fv_3 \cosh(u_3 x) \sinh(v_3(d-y)),$$

$$E_{3y} = -\frac{\mathrm{j}\beta}{\gamma_2^2} Ev_3 \cosh(u_3 x) \cosh(v_3(d-y)) - \frac{\mathrm{j}\omega\mu_0}{\gamma_2^2} Fu_3 \sinh(u_3 x) \cosh(v_3(d-y)),$$

$$H_{3x} = \frac{\mathrm{j}\omega\varepsilon_2}{\gamma_2^2} Ev_3 \cosh(u_3 x) \cosh(v_3(d-y)) + \frac{\mathrm{j}\beta}{\gamma_2^2} Fu_3 \sinh(u_3 x) \cosh(v_3(d-y)),$$

$$H_{3y} = \frac{\mathrm{j}\omega\varepsilon_2}{\gamma_2^2} Eu_3 \sinh(u_3 x) \sinh(v_3(d-y)) - \frac{\mathrm{j}\beta}{\gamma_2^2} Fv_3 \cosh(u_3 x) \sinh(v_3(d-y)). \tag{4}$$

4) In region IV ($a < x < c$ and $b < y < d$):

$$E_{4z} = G \sinh(u_4(c-x)) \sinh(v_4(d-y)),$$

$$H_{4z} = H \cosh(u_4(c-x)) \cosh(v_4(d-y)),$$

$$E_{4x} = -\frac{\mathrm{j}\beta}{\gamma_2^2} Gu_4 \cosh(u_4(c-x)) \sinh(v_4(d-y)) - \frac{\mathrm{j}\omega\mu_0}{\gamma_2^2} Hv_4 \cosh(u_4(c-x)) \sinh(v_4(d-y)),$$

$$E_{4y} = -\frac{\mathrm{j}\beta}{\gamma_2^2} Gv_4 \sinh(u_4(c-x)) \cosh(v_4(d-y)) + \frac{\mathrm{j}\omega\mu_0}{\gamma_2^2} Hu_4 \sinh(u_4(c-x)) \cosh(v_4(d-y)),$$

$$H_{4x} = \frac{\mathrm{j}\omega\varepsilon_2}{\gamma_2^2} Gv_4 \sinh(u_4(c-x)) \cosh(v_4(d-y)) - \frac{\mathrm{j}\beta}{\gamma_2^2} Hu_4 \sinh(u_4(c-x)) \cosh(v_4(d-y)),$$

$$H_{4y} = -\frac{\mathrm{j}\omega\varepsilon_2}{\gamma_2^2} Gu_4 \cosh(u_4(c-x)) \sinh(v_4(d-y)) - \frac{\mathrm{j}\beta}{\gamma_2^2} Hv_4 \cosh(u_4(c-x)) \sinh(v_4(d-y)). \tag{5}$$

Where *A, B, C, D, E, F, G,* and *H* in Eqs.(2), (3), (4), and (5) are the amplitude constants.

2.3. Boundary conditions and the 'hot' dispersion equation

By using the 'sheath helix' model,[13] the boundary conditions at the interfaces are represented as follows:

1) The tangential components of electric field are continuous at $x = a$ and $y = b$.

$$\int_{-b}^{b} E_{1z} \mid_{x=a} \mathrm{d}y = \int_{-b}^{b} E_{2z} \mid_{x=a} \mathrm{d}y, \tag{6}$$

$$\int_{-b}^{b} E_{1y} \mid_{x=a} \mathrm{d}y = \int_{-b}^{b} E_{2y} \mid_{x=a} \mathrm{d}y, \tag{7}$$

$$\int_{-a}^{a} E_{1z}\,|_{y=b}\,\mathrm{d}x = \int_{-a}^{a} E_{3z}\,|_{y=b}\mathrm{d}x\,, \tag{8}$$

$$\int_{-a}^{a} E_{1x}\,|_{y=b}\mathrm{d}x = \int_{-a}^{a} E_{3x}\,|_{y=b}\,\mathrm{d}x, \tag{9}$$

2) The electric field components along the helix direction are zero.

$$\int_{-b}^{b} (E_{1z}\sin\psi\,|_{x=a} + E_{1y}\cos\psi\,|_{x=a})\mathrm{d}y = 0, \tag{10}$$

$$\int_{-a}^{a} (E_{1z}\sin\psi\,|_{y=b} - E_{1x}\cos\psi\,|_{y=b})\mathrm{d}x = 0, \tag{11}$$

3) Because of the singular behaviour of the fields at the corners, the boundary conditions for magnetic fields in differential form cannot be used at the boundary among region I, region II and region III. Here, the chosen matching condition is that the average value of the magnetic field components are continuous along the helix direction, which result in the following integral equation:

$$\begin{aligned}&\int_{-b}^{b} (H_{1z}\sin\psi\,|_{x=a} + H_{1y}\cos\psi\,|_{x=a})\mathrm{d}y\\ &\quad+\int_{-a}^{a} (H_{1z}\sin\psi\,|_{y=b} - H_{1x}\cos\psi\,|_{y=b})\mathrm{d}x\\ &=\int_{-b}^{b} (H_{2z}\sin\psi\,|_{x=a} + H_{2y}\cos\psi\,|_{x=a})\mathrm{d}y\\ &\quad+\int_{-a}^{a} (H_{3z}\sin\psi\,|_{y=b} - H_{3x}\cos\psi\,|_{y=b})\mathrm{d}x.\end{aligned} \tag{12}$$

4) At $x = c$ and $y = d$, the field expressions already satisfy the metallic boundary conditions.

Substituting the field expressions of each region into the above boundary conditions to eliminate the amplitude constants, we can obtain the 'hot' dispersion equation for the transverse- antisymmetric modes of the rectangular helix slow-wave structure filled completely with a beam,

$$\begin{aligned}&\frac{k_1^2\cot^2\psi}{(\beta^2-k_1^2)^2} = \coth(p_u a)\frac{M}{N},\\ &p_u\tanh(p_u a) = p_v\tanh(p_v b).\end{aligned} \tag{13}$$

Where

$$\begin{aligned}M =\ & \cosh(p_u a)\sinh(p_v b)\frac{1}{p_u p_v} + \sinh(p_u a)\cosh(p_v b)\frac{1}{p_u^2} + \frac{1}{\varepsilon_{\mathrm{e}}}\coth(u_2(c-a))\sinh(p_u a)\sinh(v_2 b)\frac{1}{u_2 v_2}\\ &+\frac{1}{\varepsilon_{\mathrm{e}}}\coth(v_3(d-b))\sinh(p_v b)\sinh(u_3 a)\frac{p_v}{p_u u_3 v_3},\\ N =\ & \sinh(p_u a)\sinh(p_v b)\left(\frac{p_u^2+p_v^2}{p_u p_v}\right) + \varepsilon_{\mathrm{e}}\coth(u_2(c-a))\cosh(p_u a)\sinh(v_2 b)\frac{u_2}{v_2}\\ &+\varepsilon_{\mathrm{e}}\coth(v_3(d-b))\cosh(p_v b)\sinh(u_3 a)\frac{v_3}{u_3}.\end{aligned}$$

3. Numerical calculation and discussion

In the absence of the electron beam ($\omega_{\mathrm{p}} = 0$), the 'hot' dispersion Eq.(13) reduces to a cold dispersion equation which is consistent with that in Ref.[8]. Since the 'hot' dispersion equation (13) is a complex transcendental equation for k_0 and β, it must be resolved by numerical computation, and a general Matlab computer program has been developed to solve it. When the parameters of the electron beam and the geometry dimensions of the structure are given, the complex solution of the propagation constant β can be evaluated numerically. The small-signal gain per period can thus be obtained,

$$\begin{aligned}\mathrm{G(dB/period)} &= 20\log\{\exp[\mathrm{Im}(\beta L)]\}\\ &= 8.686\mathrm{Im}(\beta L).\end{aligned} \tag{14}$$

Where, 'Im' denotes the imaginary part of a complex number.

In order to illustrate the high gain amplification in this structure, we give several numerical results of the small-signal gain per period versus the normalized frequency according to the method described above.

Firstly the effect of the beam current I_0 on the small-signal gain is illustrated in Fig.2. It is found that for the same slow-wave structure and the same beam voltage, the gain increases and the operating bandwidth becomes wider as the beam current I_0 increases. Thus we can draw a conclusion that by en-

larging I_0, the bandwidth of rectangular helix TWT may be broadened.

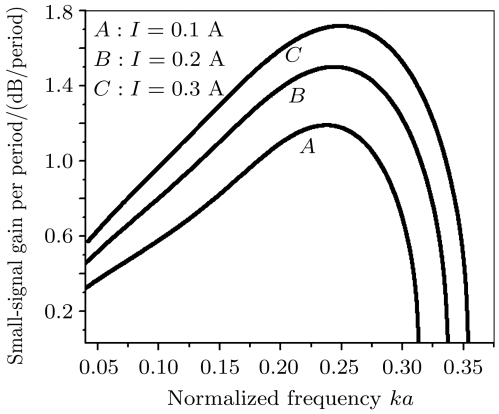


Fig.2. Effect of I_0 on the small-signal gain. Calculating parameters: $b/a = 1$, $a/L = 1$, $c/a = 2$, $d/b = 2$, $V_0 = 5$ kV, $\varepsilon_{r2} = 1.0$.

Figure 3 shows the gain for various beam voltages which approximate to the synchronous beam voltages. If the slow-wave structure parameters and the beam currents are fixed, it is obvious that operating band moves to a lower frequency range while the beam voltage increases. And the influence of the beam voltage on the gain per period is not obvious.

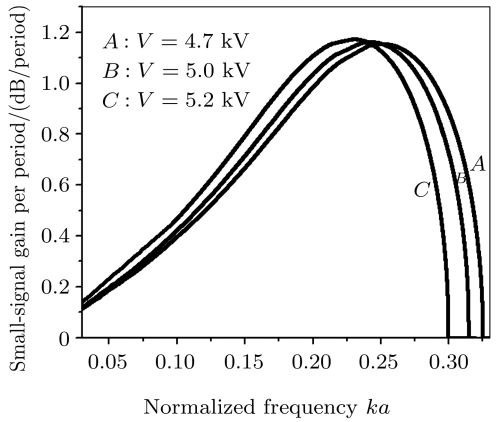


Fig.3. Effect of V_0 on the small-signal gain. Calculating parameters: $b/a = 1$, $a/L = 1$, $c/a = 2$, $d/b = 2$, $I_0 = 0.1$ A, $\varepsilon_{r2} = 1.0$.

Now, we will study the effect of the width $2b$ of the rectangular cross section on the beam-wave interaction in a small signal regime. Considering that the phase velocities of the electromagnetic waves decrease with the increase of the width when structure parameters a and L are fixed, we find that the corresponding synchronous beam voltages, which are calculated according to the electron beam line shown in the dispersion of the rectangular helix SWS (see Fig.4(a) of Ref.[8]), are therefore chosen from a large value to small one. As shown, Fig.4 is the small signal gain per period when the beam current and the parameters a and L are fixed respectively. Comparing the calculated results of the four different structures, we interestingly find that the bandwidth decreases from $b/a = 1$ to $b/a = 4$ sequentially, while the trend of the small-signal gain is opposite, the gain for $b/a = 4$ is the biggest and the gain for $b/a = 1$ is the smallest. So the rectangular helix TWT's length is reduced greatly for the high gain properties of the wider rectangular structure with the same beam current density. This indicates that the wider rectangular helix can be employed when high gain of the beam–wave interaction is required; if broad band operation is needed, the square helix should be considered.

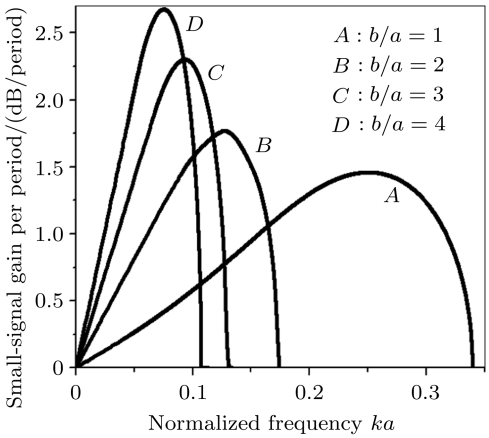


Fig.4. Comparison of the small-signal gain of four different structures. Calculating parameters: $a/L = 1$, $c/a = 2$, $d/b = 2$, $\varepsilon_{r2} = 1.0$, $I_0 = 0.2$ A. (A: $b/a = 1$, $V_0 = 5.5$ kV; B: $b/a = 2$, $V_0 = 2.5$ kV; C: $b/a = 3$, $V_0 = 1.1$ kV; D: $b/a = 4$, $V_0 = 0.6$ kV).

Figure 5 shows the small-signal for various b/a. Here parameters L and ψ in each case are the same, which means that the circumference of the rectangular cross section is constant. It is clear that, as b/a (the aspect ratio of the rectangular cross section) increases, the rectangular cross section approximates better to the planar helix case, the operating band moves to a lower frequency range and the bandwidth becomes narrow, but the gain increases while the beam voltage and beam current is fixed. Thus, the effect of b/a on the gain cannot be neglected, which accords with the analysis of a general rectangular helix SWS.[8]

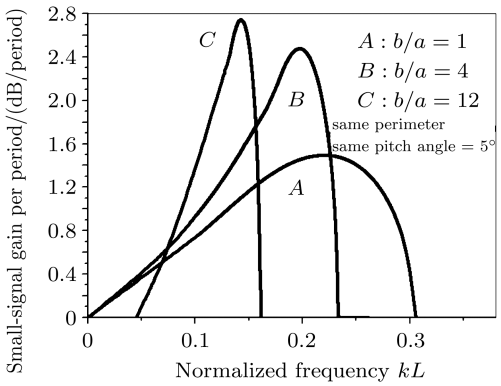


Fig.5. Effect of b/a on the small-signal gain when φ is a constant. Calculating parameters: $a + b = 6$ mm, $L = 3$ mm, $c/a = 2$, $d/b = 2$, $I_0 = 0.2$ A, $\varepsilon_{r2} = 1.0$, (A: $V_0 = 2.5$ kV, B: $V_0 = 2.3$ kV, C: $V_0 = 2.2$ kV).

For comparison with the case of the circular helix structures with comparable dispersion properties, the calculated results of the normalized phase velocity and averaged coupling impedance of the rectangular helix and the circular counterpart (both filled completely with a solid beam), which can be obtained from the dispersion equation and the coupling impedance expression in Ref.[8], are also shown in Figs.6(a) and 6(b), respectively. Figure 6(c) shows the comparison of the small signal gain between the rectangular and circular helix structures. Curves A_1 and A_2 in Fig.6(c) indicate the small-signal gain for $b/a = 1$ and its equivalent circular helix which has the same circumference and the comparable dispersion characteristics as them respectively.[8] While curves B_1 and B_2 show the small-signal gain for $b/a = 4$ and its equivalent circular helix, respectively. We can see from the curves that, the small-signal gain of the rectangular helix is bigger than the circular helix, and the wider the rectangular is, the greater the disparity. At the same time, the bandwidth keeps almost the same level of the equivalent circular helix TWT. Thus we can draw the conclusion that by employing the rectangular helix instead of the circular helix, the high gain or the compact helix TWT may be obtained.

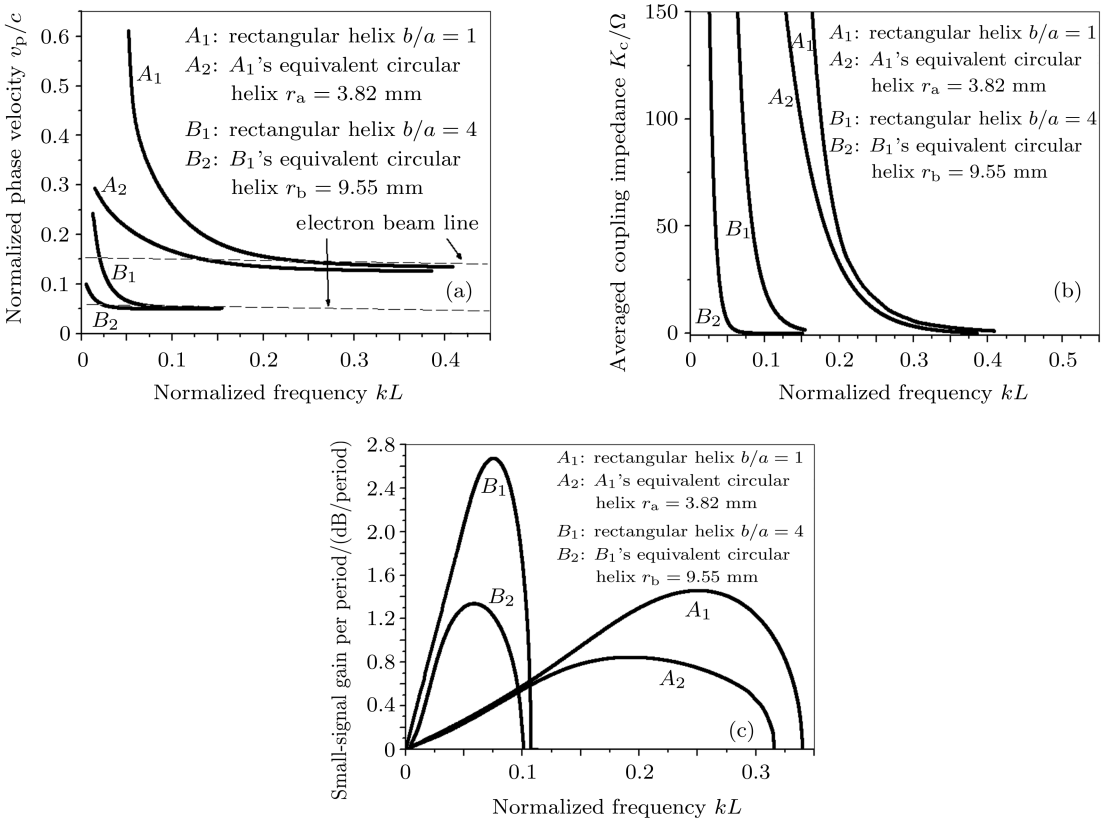


Fig.6. (a) Comparison of the normalized phase velocity for a rectangular and circular helix SWS. (b) Comparison of the averaged coupling impedance for a rectangular and circular helix SWS. (c) Comparison of the small-signal gain of rectangular and circular helix slow-wave structures. Calculating parameters: $L = 3$ mm, $a/L = 1$, $c/a = 2$, $d/b = 2$, $I_0 = 0.2$ A, $\varepsilon_{r2} = 1.0$. ($V_{A_1} = V_{A_2} = 5.5$ kV; $V_{B_1} = V_{B_2} = 0.6$ kV).

4. Conclusion

In this paper, a linear theory of the beam–wave interaction rectangular helix TWT has been investigated, and small-signal analysis is carried out. The 'hot' dispersion equation is obtained by utilizing the self-consistent field theory and then solved numerically. Also, the influence of the beam parameters and the SWS's parameters on the bandwidth and small-signal gain were investigated. The numerical results reveal that by adding the beam current, the bandwidth and the small-signal gain of rectangular helix TWT are increased; among the different rectangular helix SWSs, the gain increases and the bandwidth decreases with the increase of the width of the SWS structure whether structure parameters a and L or ψ and L are fixed or not. Also, the rectangular helix SWS can reduce the tube dimension with the higher gain than the equivalent circular helix. The analysis reveals that this kind of structure is a wide-band or high gain amplifier by choosing a proper value of the SWS and the beam parameters. The results obtained in this paper may provide a theoretical basis for designing the rectangular helix TWTs.

References

[1] Kory C, Ives L, Read M and Phillips P 2004 *Proc. 5th IEEE Int. Vacuum Electron. Conf.* p51

[2] Johnson C C 1959 *IEEE Trans. Electron Devices* **6** 189

[3] Arora R K 1966 *IEEE Trans. Antennas Propagat.* **14** 795

[4] Arora R K 1967 *Can. J. Phys.* **45** 2145

[5] Aditya S and Arora R K 1979 *IEEE Trans. Microwave Theory Tech.* 27 860

[6] Chadha D, Aditya S and Arora R K 1983 *MTT* **31** 73

[7] Chadha D, Aditya S and Aroea R K 1984 *IEE Proceedings* **131** 14

[8] Fu C F, Wei Y Y, Wang W X and Gong Y B 2008 *IEEE Trans. Electron Devices* **55** 12

[9] Fu C F, Wei Y Y, Wang W X and Gong Y B 2008 *Chin. Phys. Lett.* **25** 3478

[10] Freund H P, Kodis M A and Vanderplats N R 1992 *IEEE Trans. Electron Devices* **20** 543

[11] Lei C J, Li J Y, Liu Y H, Lou Y, Pu Y L, Wang J X and Yan R 2008 *Chin. Phys.* B **17** 460

[12] Liu P K, Su X B and Xiao L 2006 *Acta Phys. Sin.* **55** 5150 (in Chinese)

[13] Pierce J R 1950 *Traveling Wave Tubes* (New York: Van Nostrand) p21